

## Arrival Directions of Cosmic-Ray Air Showers from the Northern Sky\*

GEORGE W. CLARK

Laboratory for Nuclear Science and Department of Physics, Massachusetts Institute of Technology, Cambridge, Massachusetts

(Received June 3, 1957)

The celestial arrival directions of 2660 air showers of size greater than  $10^5$  particles at sea level have been determined with an angular resolution of  $4^\circ$ . The observations were made by the method of fast timing, and they cover a band of declination from  $10^\circ$  to  $90^\circ$  north. No significant deviation from isotropy of the primaries of these showers has been found. The response of the array to showers of various sizes and arrival directions has been evaluated theoretically and the results are given. The zenith angle dependence of the counting rate indicates an exponential attenuation with atmospheric depth of the intensity of showers at sea level with an attenuation length of  $107 \pm 11$  g cm $^{-2}$ . As a by-product of the experiment we have found a value for the absolute intensity of showers of size greater than  $10^6$  particles in the vertical direction at sea level which is  $(9.6 \pm 3.0) \times 10^{-11}$  cm $^{-2}$  sec $^{-1}$  sterad $^{-1}$ .

### INTRODUCTION

THE counting rates of nondirectional air shower detectors show little or no significant variation with sidereal time.<sup>1-4</sup> This evidence indicates that the flux of primary cosmic radiation with energies between  $10^{14}$  ev and  $10^{17}$  ev is largely independent of right ascension. However, the solid angular resolution of nondirectional air shower detectors is poor ( $\sim 1$  steradian) since it is determined only by atmospheric absorption. Consequently, the most significant results which can be obtained with such detectors are the amplitudes of the first three or four terms in a Fourier expansion of the counting rate as a function of sidereal time. A dependence of the primary flux on declination could not be detected in the data, and the effects of localized irregularities or of narrow bands of greater or lesser intensity would be obscured or lost.

For several reasons it is important to obtain more exact and detailed experimental information about the direction dependence of the primary flux. Recent developments<sup>5,6</sup> in the theory of the origin of cosmic rays have emphasized that such information can provide crucial tests of hypotheses about the magnetic fields and the cosmic-ray acceleration mechanisms in the universe. Sekido *et al.*<sup>7</sup> have found evidence from measurements with a  $\mu$ -meson telescope for the existence of a concentrated source of primaries with momenta near  $2 \times 10^{11}$  ev/c located within a solid angle  $5^\circ \times 5^\circ$  on the celestial equator. Although the existence of interstellar magnetic fields makes it highly unlikely that charged particles from a localized source in the galaxy would reach the earth from so narrow a cone of

directions, high-energy neutrons could reach the earth in straight lines from a localized source nearby as Rothwell *et al.*<sup>8</sup> have pointed out. Certain models of the propagation of cosmic rays in the galaxy lead to the prediction of a narrow band of relatively low intensity.<sup>9</sup> Finally, the sun and the moon must cast a "shadow" in the flux of high-energy primary cosmic rays and observations of this shadow effect might give new information about the magnetic fields of these bodies.

The arrival directions of individual high-energy primaries have been determined by means of unidirectional detectors with narrow apertures. The narrow-angle Geiger-Müller counter telescope,<sup>7</sup> and the shower detector with one tray shielded from all but a narrow solid angle of sky<sup>1</sup> are examples of this type of detector. Since the counting rate of a unidirectional detector obviously decreases as the angular resolution is increased, such a detector is not well suited to a random search for irregularities in the primary flux.

Two types of directional detectors with wide apertures limited only by atmospheric absorption have been used to determine the arrival directions of primaries with energies above  $10^{15}$  ev. Rothwell *et al.*<sup>8</sup> have triggered cloud chambers by a nondirectional air shower detector sensitive to showers produced by primaries with an average energy of  $8 \times 10^{15}$  ev, and they have determined the arrival directions of 1100 showers with an uncertainty between  $3^\circ$  and  $5^\circ$  by measuring the orientation of the shower particle tracks in the chambers. Bassi *et al.*<sup>10</sup> have determined the arrival directions of air showers by a method of fast timing which involves the measurement of the differences in the arrival times of the shower particles at several laterally separated detectors on the ground. Both of these methods entail a more laborious reduction of experimental data than do those employing nondirectional and unidirectional detectors. However, the method of fast timing gives data in a form which

\* This work is supported in part by the joint program of the Office of Naval Research and the U. S. Atomic Energy Commission.

<sup>1</sup> F. J. M. Farley and J. R. Storey, Proc. Phys. Soc. (London) **A67**, 996 (1954).

<sup>2</sup> T. E. Crawshaw and W. Galbraith, Phil. Mag, **45**, 1109 (1954).

<sup>3</sup> Auger, Cachon, Daudin, Freon, and Mosykowski, Compt. rend. **240**, 2407 (1955).

<sup>4</sup> J. K. Crawshaw and H. Elliot, Proc. Phys. Soc. (London) **A69**, 102 (1956).

<sup>5</sup> For a general review and list of references see B. Rossi, Suppl. Nuovo cimento **2**, 275 (1955).

<sup>6</sup> L. Davis, Phys. Rev. **96**, 743 (1954).

<sup>7</sup> Sekido, Yoshida, and Kamuja, Nature **177**, 35 (1956).

<sup>8</sup> Rothwell, Wade, and Goodings, Proc. Phys. Soc. (London) **A69**, 902 (1956).

<sup>9</sup> L. Davis (private communication).

<sup>10</sup> Bassi, Clark, and Rossi, Phys. Rev. **92**, 441 (1953).

permits, at present, a considerable mechanization in the arithmetical computations and may, in the future, permit automatic recording of the data. Consequently, it appears that this method offers a better possibility for obtaining results of high statistical significance than does the cloud chamber method which requires the stereoscopic analysis of photographs.

We shall describe a survey in the northern sky of the arrival directions of over 3000 primaries which generated extensive air showers containing more than  $10^5$  particles at sea level. The survey was made by the method of fast timing and is an extension of the earlier work described by Bassi *et al.*<sup>10</sup> In addition, we shall give experimental results on the absorption of showers in the atmosphere and on their absolute intensity.

II. DESCRIPTION OF THE METHOD

Bassi *et al.*<sup>10</sup> demonstrated that at a given instant most of the particles in an air shower lie within a thin disk that is perpendicular to the shower axis, and that moves in a direction parallel to the axis with a velocity near that of light. Since the relative arrival times of the disk at various places on the ground are simply related to the orientation of the axis, it is possible to determine the orientation from measurements of the relative arrival times of the particles. In practice these measurements can be made with scintillation detectors and fast electronic timing apparatus.

We consider first the geometrical problem of relating the observed arrival times to the orientation of the axis. It is convenient to choose a rectangular coordinate system whose  $x$ - $y$  plane is the ground and whose  $y$ -axis points north as illustrated in Fig. 1(a). We imagine an arrangement of  $n$  timing detectors spread out on the ground plane, and call  $x_i, y_i$  the rectangular coordinates of the  $i$ th detector. Let the observed arrival times of a shower disk at the  $i$ th detector be  $t_i$ . According to the observations of Bassi *et al.*, it is possible to find for each shower a hypothetical plane which moves in the direction of its normal vector  $\mathbf{k}$  with the velocity of light  $c$ , and which intersects the detectors at times which correspond closely to the observed arrival times.

The equation of this plane is

$$ct' = ct_0 - lx - my - nz, \tag{1}$$

where  $t'$  is the time of arrival of the plane at the point  $x, y, z$ . We form the function

$$\begin{aligned} \Phi^2 &= \frac{1}{n-3} \sum_{i=1}^n c^2 (t_i - t_i')^2 \\ &= \frac{1}{n-3} \sum_{i=1}^n (ct_i + lx_i + my_i - ct_0)^2, \end{aligned} \tag{2}$$

and seek those values of  $l, m,$  and  $t_0$  which minimize

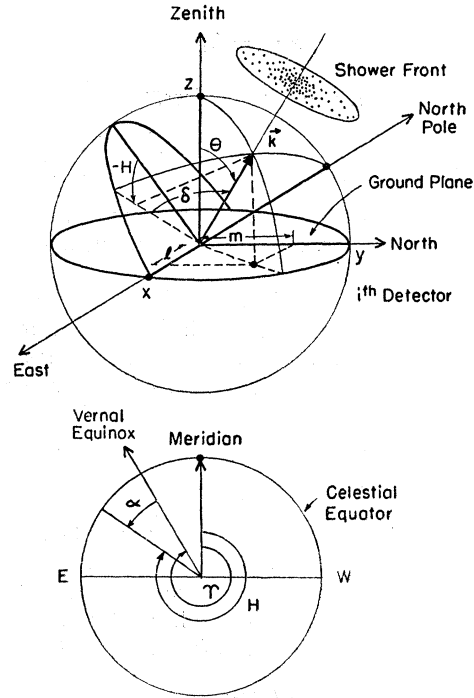


FIG. 1. (a) Schematic diagram of a shower front approaching an array of detectors. (b) Diagram of the relation between  $H, \gamma,$  and  $\alpha$ .

$\Phi^2$ , namely those values which satisfy the set of equations

$$\begin{aligned} (\sum x_i^2) + (\sum x_i y_i)m - (\sum x_i)ct_0 &= -\sum x_i ct_i, \\ (\sum x_i y_i) + \sum y_i^2 m - (\sum y_i)ct_0 &= -\sum y_i ct_i, \\ (\sum x_i) + (\sum y_i)m - nt_0 &= -\sum ct_i. \end{aligned} \tag{3}$$

The values of  $l$  and  $m$  obtained in this way are the direction cosines of the vector normal to the plane whose arrival times best fit the observed data.

The zenith angle,  $\theta$ , between the shower axis and the vertical direction is related to  $l$  and  $m$  by the equation

$$\theta = \arcsin[(l^2 + m^2)^{1/2}]. \tag{4a}$$

The azimuth  $\phi$ , measured clockwise from north, is given by

$$\begin{aligned} \phi &= \arcsin[l / (l^2 + m^2)^{1/2}] \\ &= \arcsin[m / (l^2 + m^2)^{1/2}]. \end{aligned} \tag{4b}$$

In order to express the orientation in terms of the declination,  $\delta$ , and the right ascension,  $\alpha$ , we define the following additional quantities:  $\gamma$ =local sidereal time (hour angle of vernal equinox),  $L$ =local longitude,  $\delta_0$ =local latitude,  $T_1, T_2$ =local standard time in hours and minutes,  $\eta$ =the number of time zones west of Greenwich,  $D$ =number of days since December 31,  $\gamma_0$ =right ascension of the vernal equinox at midnight on December 31 at Greenwich, and  $H$ =hour angle of arrival direction. Then

$$\delta = \arcsin\{m \cos \delta_0 + (1 - l^2 - m^2)^{1/2} \sin \delta_0\}, \tag{5a}$$

and

$$\alpha = \gamma - H, \tag{5b}$$

where

$$H = -\arcsin(l/\cos\delta), \tag{5c}$$

and

$$\gamma = \gamma_0 - L + 15\eta + 0.986D + 15.041(T_1 + 0.0167T_2). \tag{5d}$$

The relation between  $\alpha$ ,  $H$ , and  $\gamma$  is shown schematically in Fig. 1(b). The various numerical quantities are derived from astronomical data on the angular velocity of the rotation of the earth on its axis and the revolution of the earth about the sun. The coefficient of  $D$  is assumed to be constant although strictly speaking, it varies by about 0.05% around its average value because the angular velocity of the earth about the sun depends upon the time of year.

### III. EXPERIMENTAL ARRANGEMENT

The principle of fast-timing measurements expressed by Eqs. (2) and (3) is applicable to any array of detectors. In the present survey we used four detectors in a square array. If the square has sides of length  $d$ , then the values of  $l$  and  $m$  which minimize  $\Phi^2$  are

$$l = c(t_3 + t_4 - t_1 - t_2)/2d, \tag{6a}$$

and

$$m = c(t_2 + t_4 - t_1 - t_3)/2d. \tag{6b}$$

With these values of  $l$  and  $m$ , the function  $\Phi^2$  is reduced to its minimum value

$$\Phi^2 = \Delta^2/4,$$

where we have placed

$$\Delta = c(t_1 + t_4 - t_2 - t_3). \tag{6c}$$

These values are used in Eqs. (4) and (5) for the computation of the zenith angle, declination, and right ascension of the shower axis.

Only a brief description of the timing apparatus used in this survey will be given. A description of an improved version will be published elsewhere.

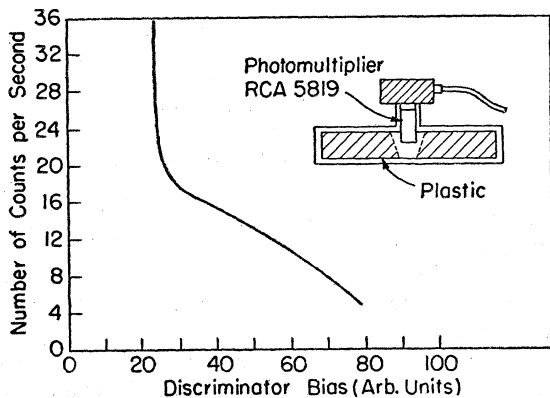


FIG. 2. Integral size distribution of pulses from plastic scintillation detector exposed to cosmic rays at sea level, and schematic diagram of the detector.

The detectors used in a part of this survey were cylindrical scintillation detectors with liquid scintillators composed of toluene, *p*-terphenyl (3 g/l), and popop (10 mg/l). A considerable improvement in efficiency and convenience was achieved when these were later replaced by plastic scintillation detectors that have been described elsewhere.<sup>11</sup> The plastic fluors were 2½ in. × 16 in. cylinders. The optical arrangement of the plastic scintillation detectors is shown in Fig. 2, together with the integral size distribution of pulses from the detector. The "plateau" is produced by the uncollimated flux of fast cosmic-ray particles passing through the detector. The high voltage was supplied to the photomultipliers through the same cable that carried the pulses from the collecting anode of the multiplier to the central station.

At the central station the pulses were artificially delayed with respect to one another by fixed delay lines, added, amplified by distributed line amplifiers, and displayed on the vertical deflection of a fast

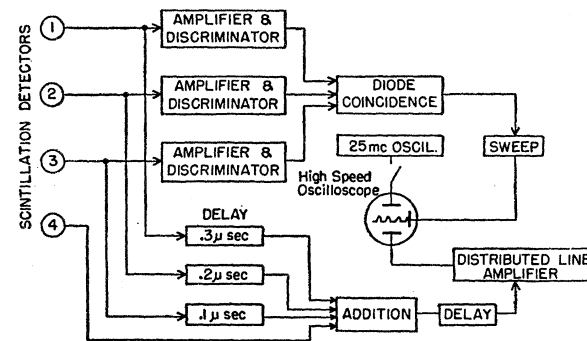


FIG. 3. Block diagram of the electronic circuits.

oscilloscope. The sweep of the oscilloscope was triggered by a coincidence of pulses between detectors 1, 2, and 3 within 200  $\mu\text{sec}$ . Single minimum-ionizing particles traversing each of these detectors were sufficient to trigger the apparatus and produce readable pulses. Only those events which showed a fourth pulse from detector 4 on the sweep were analyzed. Figure 3 is a block diagram of the electronic equipment.

For the determination of arrival directions, we measured the relative positions of the starting points of the pulses (corresponding to the arrival times at each detector of the first of possibly several particles) on the projected image of the oscillogram. An event which struck all four detectors simultaneously gave a pattern of four pulses whose relative positions on the sweep were determined by the fixed delays in the cables and delay lines. Differences in the arrival times of particles at the detectors could then be determined from measurements of the changes in the pattern. We determined the relative positions for simultaneous pulses by stacking the four detectors on top of one

<sup>11</sup> Clark, Scherb, and Smith, Rev. Sci. Instr. 28, 433 (1957).

another and measuring the pulses from particles (mostly  $\mu$  mesons) which traversed the entire stack. Appropriate corrections were made for the time of flight of the particles. The sweep speed was determined with a crystal controlled 25-Mc oscillator. The data on the positions of the pulses along with the date, time of observation, and sweep speed were transferred to IBM cards. The computation of  $\Delta$ ,  $\theta$ ,  $\varphi$ ,  $\delta$ , and  $\alpha$  were carried out on an IBM 650 computer and the analysis of the results was then completed on automatic card sorting machines.

IV. EXPERIMENTAL RESULTS

A. Angular Resolution

If the particles which produce the four pulses in an event lay exactly in a plane perpendicular to the shower axis, and if the measurements of the relative arrival times of the pulses were free of experimental errors, the determination of the direction cosines of the axis would be exact, and the value of  $\Delta$  would be zero. Lack of perfect coplanarity of the shower particles and random experimental errors both produce similar fluctuations in  $l$ ,  $m$ , and  $\Delta$ . We shall therefore use the observed distribution of  $\Delta$  to estimate the uncertainties in the measurement of  $l$  and  $m$ .

We call  $\tau_i$  the difference between the observed arrival time  $t_i$  and the corresponding arrival time  $t'_i$  of the moving plane which best fits the data. The  $\tau_i$ 's in each event are, to a certain extent, correlated with one another in a complex way which depends on the detailed characteristics of the shower such as the lateral distribution, the core location, the size, and the arrival direction. If they were, instead, random independent variables, we could relate the dispersions of  $l$ ,  $m$ , and  $\Delta$  by the equation

$$D(l) = D(m) = 4D(\tau) / 4d^2 = D(\Delta) / 4d^2,$$

where  $D(x)$  represents the statistical dispersion of the variable  $x$ . We shall make the crude approximation that this relation is valid in the actual case.

Figure 4 is a plot of  $\Delta$  for 3000 unselected showers and from these data we derive a value for  $[D(\Delta)]^{1/2}$  which is

$$[D(\Delta)]^{1/2} = 5.1 \text{ meters.}$$

It follows that we would expect to find for the standard deviation of measurements of  $l$  or  $m$  on a set of unselected showers the approximate value

$$[D(l)]^{1/2} = [D(m)]^{1/2} = [D(\Delta)]^{1/2} / 2d = 0.070.$$

This corresponds to a resolution in  $\theta$  of  $\pm 5^\circ$  for vertical unselected showers. We increased the effective resolution of the instrument by rejecting events in which  $|\Delta|$  exceeded 6.4 meters so that for showers selected according to this criterion the resolution in  $\theta$  is about  $\pm 4^\circ$ , and the solid angular resolution is about 40 square degrees.

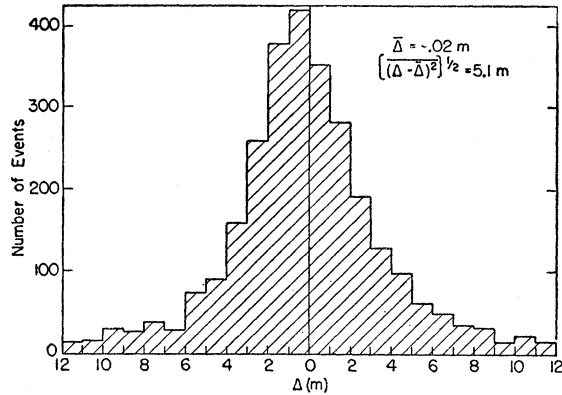


FIG. 4. Histogram plot of the distribution of  $\Delta$ .

The contributions of purely instrumental and reading errors to the distribution of  $\Delta$  were determined from measurements with the detectors in a vertical stack. Most events recorded with this arrangement were produced by relativistic particles traversing the stack so that the only cause of fluctuations in the measured relative positions of the pulses were instrumental and reading errors. We found for these events

$$[D(\Delta)]^{1/2} = 1.0 \text{ meter,}$$

and this indicates that the effect of these errors on direction measurements is negligible compared to the effect of the noncoplanarity of shower particles.

B. Size Distribution

We define the size  $N$  of a shower to be the total number of ionizing shower particles which arrive at sea level with sufficient energy to register in our detectors. Although  $N$  is, strictly speaking, a discontinuous variable, it is always a very large integer for the showers we record, so that it is convenient to consider it to be a continuous variable. We have calculated the distribution in size of the showers recorded with our detector array in order to evaluate their absolute intensity and to estimate the range of energies of the primary particles which produce them.

Let  $K(N, \theta) d\Omega dA$  represent the absolute rate of showers at sea level with sizes greater than  $N$  whose cores strike within the area  $dA$ , and which arrive from the solid angle  $d\Omega$  near the zenith angle  $\theta$ . Call  $s(N, \theta) \times dN d\Omega$  the rate at which showers are recorded with sizes between  $N$  and  $N + dN$  from zenith angles near  $\theta$  and in the solid angle  $d\Omega$ . We shall relate  $s$  to  $K$  on the basis of the following assumptions:

(1) The average number of particles which traverse an area  $dA$  perpendicular to a shower axis at a distance  $r$  from the axis is

$$f(r) dA = \frac{N}{2\pi} \left( \frac{e^{-r/r_0}}{r_0} \right) dA, \tag{7}$$

where  $r_0 = 79$  meters.

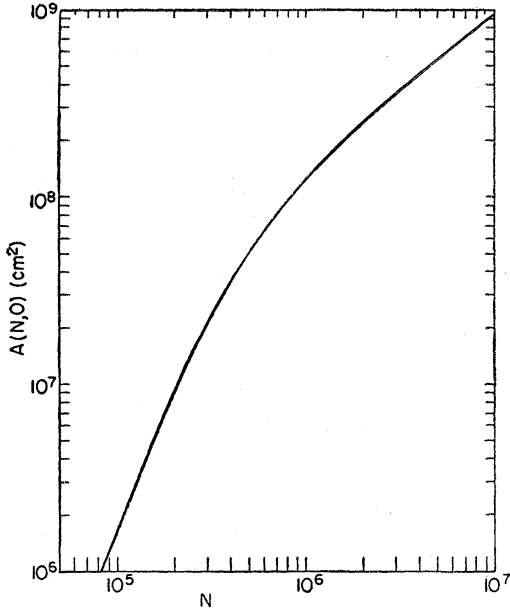


FIG. 5. Plot of projected effective area for the detection of showers at vertical incidence.

(2) The absolute intensity is

$$K(N, \theta) = K(\theta) (N/10^6)^{-\Gamma(N)}, \quad (8)$$

where  $\Gamma(N) = 1.53 + 0.0195 \ln(N/10^6)$ .

Out to distances of about  $r = 300$  meters the lateral distribution given by Eq. (7) agrees well with the results of several different experiments,<sup>12,13</sup> and is a good approximation to the theoretical distribution for pure photoelectronic showers calculated by Nishimura and Kamata for the age parameter  $S = 1.4$ .<sup>12</sup> The separation of the zenith angle dependence and the size dependence in Eq. (8) is an approximation which is justified by the experimental observation that the rate of attenuation of the intensity of showers with increasing depth in the atmosphere and, correspondingly, the zenith angle distribution, change very slowly with shower size.<sup>13</sup> The size dependence of the intensity is that obtained by Greisen<sup>12</sup> from an analysis of the local density spectrum of air showers as measured with Geiger tubes.

We call  $\epsilon(N, \theta, \rho, \alpha, \phi)$  the probability for the detection of a shower of size  $N$  whose axis is oriented in the direction specified by  $\theta$  and  $\phi$ , and intersects the ground at the position with polar coordinates  $\rho$  and  $\alpha$ , and we define the quantity  $A(N, \theta)$  by the relation

$$A(N, \theta) = \cos\theta \int_0^\infty d\rho \int_0^{2\pi} \rho d\alpha \int_0^{2\pi} \epsilon(N, \theta, \rho, \alpha, \phi) d\phi. \quad (9)$$

<sup>12</sup> K. Greisen, *Progress in Cosmic-Ray Physics*, edited by J. G. Wilson (North Holland Publishing Company, Amsterdam, 1956), Vol. III, Chap. 1.

<sup>13</sup> Clark, Earl, Kraushaar, Linsley, and Scherb, *Nature* **180**, 353 (1957).

$A(N, \theta)$  is the effective projected area for the detection of showers of size  $N$  which arrive from zenith angle  $\theta$ . The relation between  $K$  and  $s$  is then

$$s(N, \theta) = -\frac{\partial K}{\partial N} A(N, \theta). \quad (10)$$

The effective triggering requirement for the array was a fourfold coincidence among the detectors. Therefore, the expression for  $\epsilon$  is

$$\epsilon(N, \theta, \rho, \alpha, \phi) = \prod_{i=1}^4 \{1 - e^{-a(\theta)f(N, r_i)}\}, \quad (11)$$

where  $r_i$  is the perpendicular distance from the axis to the  $i$ th detector, and  $a(\theta)$  is the projected area of the  $i$ th detector on a plane perpendicular to the axis. We can write for  $r_i$  the expression

$$r_i = \{(\rho \sin\alpha - x_i)^2 + (\rho \cos\alpha - y_i)^2 - \sin^2\theta\}^{1/2} \times (\sin\phi[\rho \sin\alpha - x_i] + \cos\phi[\rho \cos\alpha - y_i]), \quad (12)$$

and for  $a(\theta)$  the expression

$$a(\theta) = \pi p^2 \cos\theta + 2pq \sin\theta, \quad (13)$$

where  $p$  is the radius of the scintillators and  $q$  is their thickness.

We evaluated  $A(N, \theta)$  for several values of  $N$  and for values of  $\theta$  equal to  $0^\circ$ ,  $32^\circ$ , and  $45^\circ$  by combining Eqs. (7), (9), (11), (12), and (13), and carrying out the integrations numerically on an automatic electronic digital computer. A plot of the results for  $\theta = 0^\circ$  is shown in Fig. 5. The corresponding plots for  $\theta = 32^\circ$  and  $45^\circ$  do not differ by more than 6% from this one for any of the calculated points. According to our assumption that the size dependence of the absolute intensity is the same for all zenith angles, it follows that the shape of the size distribution is nearly independent of the zenith angle, and that the size distribution of recorded vertical showers will be nearly the same as the size distribution of all recorded showers. Combining the calculated values of  $A(N, 0)$  with the assumed form of  $K(N, 0)$  according to Eq. (10), we obtain the size distribution  $s(N, 0)$  shown in Fig. 6 which indicates that the most probable size of showers detected in this experiment was  $1.5 \times 10^6$  particles. The corresponding value for the most probable energy of the primary particles is about  $10^{15}$  ev.<sup>13</sup>

### C. Zenith Angle Distribution

Information about the absorption of showers in the atmosphere can be obtained from an analysis of the zenith angle distribution of showers recorded with our array. For this analysis it is convenient to replace the variable  $\theta$  in Eq. (8) by  $x = x_0/\cos\theta$ , which represents the amount of atmosphere traversed by a shower arriving at the depth  $x_0$  ( $x_0 = 1040$  g cm<sup>-2</sup> at sea level) from the zenith angle  $\theta$ . We now make the assumption

that  $K$  is an exponentially decreasing function of  $x$  with an absorption length  $\Lambda$ . Furthermore, for the sake of simplicity, we shall ignore the slight variation of  $\Gamma$  with  $N$  and take it to be constant and equal to its value for  $N=10^6$ . We then have

$$K(N, x) = K_0(N/10^6)^{-1.53} e^{-(x-x_0)/\Lambda}. \quad (14)$$

Let  $R(x)$  represent the counting rate for showers of all sizes which arrive from zenith angles greater than  $\theta = \arccos(x_0/x)$ . This is the quantity which we measure directly, and it is related to  $s$  (and thereby to  $K$  and  $A$ ) by the equation

$$R(x) = 2\pi \int_x^{x_0} \frac{x_0}{x'^2} \left\{ \int_0^\infty s(N, x') dN \right\} dx', \quad (15)$$

where  $2\pi(x_0/x'^2)dx' = 2\pi \sin\theta' d\theta' = d\Omega$  is the element of solid angle. From Eqs. (10), (14), and (15), it follows that

$$\frac{1}{\Lambda} = -\frac{d}{dx} \left\{ \ln \frac{dR}{d\Omega} \right\} + \left( \int_0^\infty N^{-2.53} \frac{\partial A}{\partial x} dN / \int_0^\infty N^{-2.53} A dN \right). \quad (16)$$

We evaluated the first term on the right side of Eq. (16) from the observed relative frequencies of showers per unit solid angle in successive equal intervals of  $x$ . Figure 7 is a semilogarithmic plot of the data. The straight line in the figure was fitted to the data for  $(x-x_0) < 160 \text{ g cm}^{-2}$  by the method of least squares. Data for  $(x-x_0) > 160 \text{ g cm}^{-2}$  were not included because of the increasingly important effect of experimental errors on the determination of  $x$ . The logarithmic

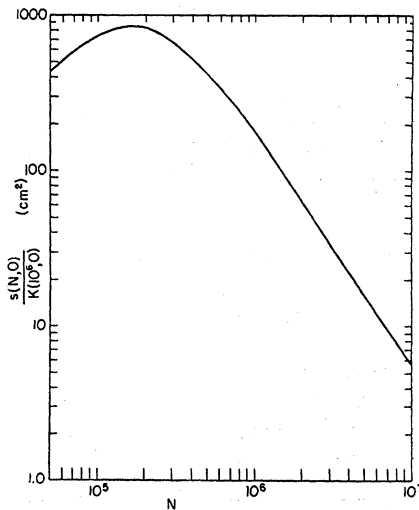


FIG. 6. Distribution in size of showers recorded at vertical incidence.

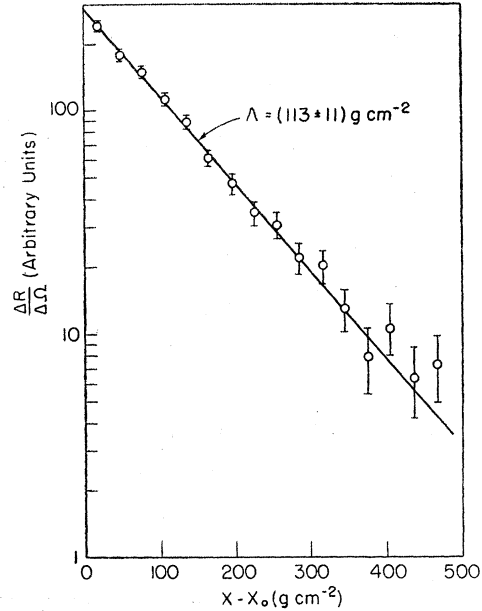


FIG. 7. Plot of shower intensity versus atmospheric depth as derived from the observed distribution in zenith angle.

slope of the line is  $8.85 \times 10^{-3} \text{ g}^{-1} \text{ cm}^2$ , and the good quality of the fit, even for  $(x-x_0) > 160 \text{ g cm}^{-2}$ , indicates the validity of the assumption of an exponential depth dependence as expressed by Eq. (14). We evaluated the last term in Eq. (16) from the results of the numerical calculation described in Sec. B, and since it was found to be less than  $2 \times 10^{-4} \text{ g}^{-1} \text{ cm}^2$  it will be neglected. Random errors in the determination of the arrival directions tend to broaden slightly the observed zenith-angle distribution. A rough estimate of this effect indicates that a correction of about 5% should be applied to the measured slope. The final value obtained for the attenuation length of the shower intensity is

$$\Lambda = 107 \pm 11 \text{ g cm}^{-2}.$$

This result may be compared to that derived from an analysis of the barometric coefficients and the attitude variation of showers by Greison.<sup>12</sup> At altitudes above sea level he obtained the value  $133 \text{ g cm}^{-2}$  for the attenuation length of the intensity of showers with more than about  $10^6$  particles. Although the experimental methods on which the two values are based are very different, we are not aware of a systematic error in either method which would explain so large a discrepancy. Small differences may arise from the difference in the contribution of unstable particles to shower development along vertical and slanted paths through the atmosphere, and from the fact that our measurements were made for atmospheric thickness greater than the vertical depth at sea level.

A quantity of more direct physical interest than  $\Lambda$  is the attenuation length,  $\lambda$ , for the number of particles

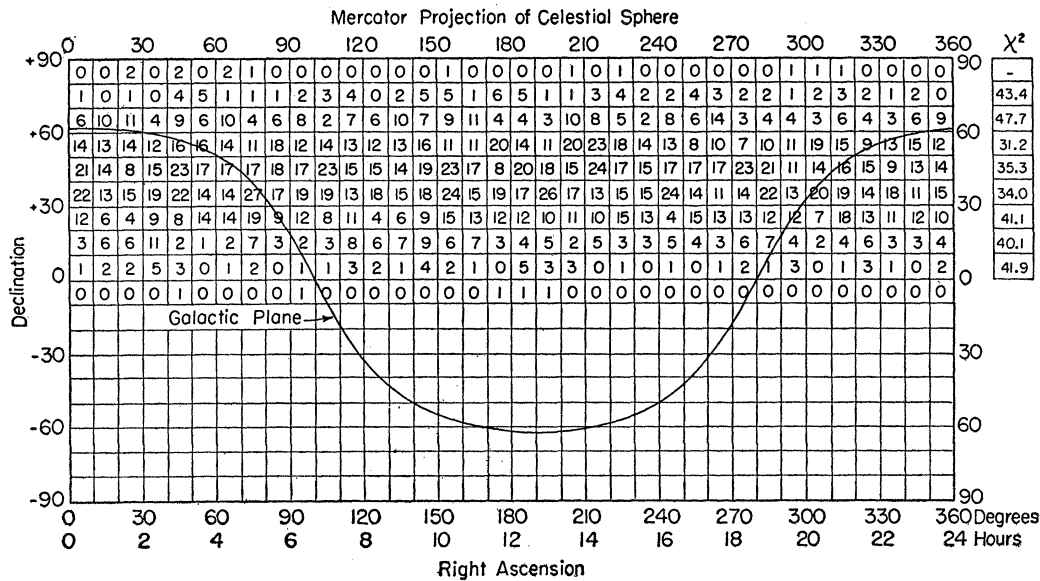


FIG. 8. Numbers of events observed within  $10^\circ \times 10^\circ$  areas on a Mercator projection of the celestial sphere.

in individual showers. We define  $\lambda$  by

$$\frac{1}{\lambda} = - \left[ \frac{1}{N} \left( \frac{\partial N}{\partial x} \right) \right]_{K=\text{constant}}$$

If we assume Eq. (14) to be valid, then  $\lambda$  is related to  $\Lambda$  and  $\Gamma$  by

$$\lambda = \Gamma \Lambda.$$

Using the measured value for  $\Lambda$  and taking  $\Gamma = 1.53$ , we find

$$\lambda = (164 \pm 17) \text{ g cm}^{-2}.$$

#### D. Absolute Intensity of Showers

Although the present experiment was not designed for the purpose of measuring the absolute intensity of showers, we have obtained as a by-product a value for this quantity by finding the value of the constant  $K_0$  in Eq. (14) which gives an expected counting rate according to Eq. (15) that is equal to the observed counting rate for showers of all sizes and all arrival directions. The observed rate is  $(113 \pm 10) \text{ day}^{-1}$  and the corresponding value for  $K_0$  is  $(3.0 \pm 1.0) \times 10^{-12} \text{ cm}^{-2} \text{ sec}^{-1} \text{ sterad}^{-1}$ . The indicated error reflects the uncertainties in the determination of the observed rate and in the values of  $\Gamma$ ,  $\Lambda$  and the effective area. From this result we find that the intensity of showers of size greater than  $10^6$  particles is  $(9.6 \pm 3.0) \times 10^{-11} \text{ cm}^{-2} \text{ sec}^{-1} \text{ sterad}^{-1}$ . The corresponding value obtained by Greisen<sup>12</sup> is  $(17 \pm 4) \times 10^{-11} \text{ cm}^{-2} \text{ sec}^{-1} \text{ sterad}^{-1}$ . It should be noted that the difference between these values could be accounted for by a discrepancy of 50% between the determination of shower "size" by Geiger tube density measurements and by the method used in the present experiment.

#### E. Distribution of Celestial Arrival Directions

The apparatus was turned off occasionally in order to change film and make repairs. In order to evaluate the distribution in celestial arrival directions it was necessary, therefore, to make proper allowance for the different numbers of days on which the apparatus was operating at various sidereal times. We first made a plot of the number of days on which the apparatus was running *versus* sidereal time. We then rejected data during various "over-exposed" sidereal time intervals selected at random from enough days to smooth out this plot to its lowest level.

The data, corrected for exposure time in this way, are summarized in Fig. 8 which is a Mercator projection of the celestial sphere. We have indicated the number of events observed in solid angle elements bounded by parallels of declination and great circles of right ascension separated in both cases by  $10^\circ$  intervals. The variation of the average barometric pressure with sidereal time was small. Furthermore, the barometric correction for a given sidereal time is spread out over an interval of about  $50^\circ$  in right ascension since showers from approximately this interval in right ascension contribute to the recorded rate at any given sidereal time. Since the net barometric correction was small compared to the statistical fluctuations, it was ignored.

We have applied several statistical tests in order to determine whether the hypothesis of an isotropic primary flux is consistent with our observations. These tests were selected because of certain preconceived notions as to the possible nature of anisotropies which one might possibly find in the primary flux, namely: (a) general lumpiness, (b) isolated regions in which the intensity is greater or less than average ("point"

sources or shadows), and (c) connected regions of more or less than average intensity corresponding to certain directions in space (e.g., the galactic equator).

We have tested for general lumpiness by applying the  $\chi^2$  test to the data from each of the  $10^\circ$  bands of declination. The largest value of  $\chi^2$  obtained for the 8 bands between  $\delta=0^\circ$  and  $\delta=80^\circ$  was 47.7 and the probability that  $\chi^2$  should have exceeded this value for one or more of the bands is 56%. The numerical results are indicated in Fig. 7.

The above test already indicates the absence of any pronounced point source in the band of declinations from  $20^\circ\text{N}$  to  $70^\circ\text{N}$ . However, it is useful to compute the probability of having seen a deviation from the mean as great as the greatest actually observed in the region of sky bounded by  $20^\circ < \delta < 60^\circ$ . The greatest positive deviation occurs in the patch of sky bounded by

$$210 < \alpha < 220, \quad 50 < \delta < 60.$$

The greatest negative deviation is seen in the patch bounded by

$$20 < \alpha < 30, \quad 40 < \delta < 50.$$

If we approximate the distribution of the numbers of events within the  $10^\circ \times 10^\circ$  areas along a given declination interval by a Gaussian distribution, the probability of having seen deviations as great as these is 60% for the positive deviation, and 92.5% for the negative deviation.

We have tested for anisotropies of the type listed

TABLE I. Expected and observed numbers of showers from several special regions of the sky.

	Expected	Observed
Galactic equator	996	972
Perpendicular to spiral arm	945	968
Along the spiral arm ( $\alpha=300^\circ$ , $\delta=35^\circ$ )	325	297

under (c) above in the three cases of the galactic equator, the plane perpendicular to the spiral arm, and the direction along the spiral arm. We drew projections of the galactic equator and of the plane and normal to the axis of the local arm of the galactic spiral.<sup>6</sup> In both cases we counted the number of events which occurred in the  $10^\circ \times 10^\circ$  patches which contained points within  $20^\circ$  of the projected plane. Similarly, we counted the number of showers in the  $10^\circ \times 10^\circ$  patches which contained points within  $20^\circ$  of the direction along the spiral arm.<sup>6</sup> We compared these numbers with the numbers expected on the basis of the average values obtained in each declination interval. The results were as shown in Table I. In all three cases the expected and observed numbers do not differ significantly from one another.

On the basis of these tests we conclude that our data do not indicate any deviation from isotropy of the flux of primaries of showers with more than  $10^5$  particles at sea level. The same conclusion has been reached by Rothwell *et al.*<sup>8</sup> from their data, although the present results are based on more than twice as many shower events.